Mass-Transfer Enhancement in Single-Drop Extraction Experiments

Martin Henschke and Andreas Pfennig
Lehrstuhl für Thermische Verfahrenstechnik, RWTH Aachen, Wüllnerstrasse 5, D-52056 Aachen, Germany

To reduce costs, engineers in the industry wish to substitute laboratory-scale experiments for pilot-scale investigations. Thus mass-transfer experiments with single drops seem to be a first step toward the design of liquid–liquid extraction columns, along with other experiments needed, for example, for the estimation of coalescence parameters.

In this article it is shown that it is possible to describe nonstationary mass transfer between single drops and a continuous phase with a single parameter, the instability constant C_{IP}. The instability constant is independent of both drop diameter and contact time between drop and continuous phase. Thus in principle a single laboratory experiment allows the determination of C_{IP} for a given combination of components. When mass transfer in an extraction column is calculated using the estimated value of C_{IP}, an increase in mass transfer due to the concentration gradient in the continuous phase of the column has to be accounted for appropriately.

Introduction

Today safe design of technical columns for liquid–liquid extraction requires experiments on a pilot-plant scale. Such testing is time-consuming and expensive. Thus, industry is very interested in minimizing experiments on a pilot-plant scale and to substitute laboratory-scale experiments or even simulations instead (Schröter et al., 1998).

To achieve this goal, mathematical models for the description of mass transfer, backmixing, breakage, coalescence, and drop motion in a column are needed. Because it does not yet seem possible to use models without experimentally estimated parameters, it would be useful if the estimation of the parameters could be done using laboratory-scale experiments.

As a first step we focused on mass transfer. Two measuring cells for laboratory experiments have been designed in close collaboration with industry. One of the cells is used for the measurement of drop velocity during sedimentation as a function of drop diameter when mass transfer occurs simultaneously (that is, equipment similar to that used by Hoting, 1996). The second cell allows the determination of the mass-transfer rate as a function of drop diameter, concentration of transferred component, and residence time of the drop in the continuous phase (see Schröter et al., 1998, for a detailed description).

Evaluating the results obtained in these cells and transferring them to extraction columns requires answering the following questions that strongly affect the reliability of the column simulations:

1. An acceptable experimental effort only allows a limited number of selected data points to be measured with the cells. Typically, the residence time can be varied while the drop diameter is kept constant or vice versa. How can these data then be interpolated or extrapolated in a physically significant way so as to predict the behavior for arbitrary drop diameters and residence times in the columns?
2. In both measuring cells the concentration of the transfer component in the continuous phase remains nearly constant during an experiment while droplets in a column pass through a concentration gradient. How will this difference in boundary conditions affect the mass transfer?

This report answers these questions in detail based on the results of experiment and simulation. Thus, this work will help the development engineer to get a first idea about the mass-transfer characteristics of a refined combination of components.

Correspondence concerning this article should be addressed to M. Henschke.

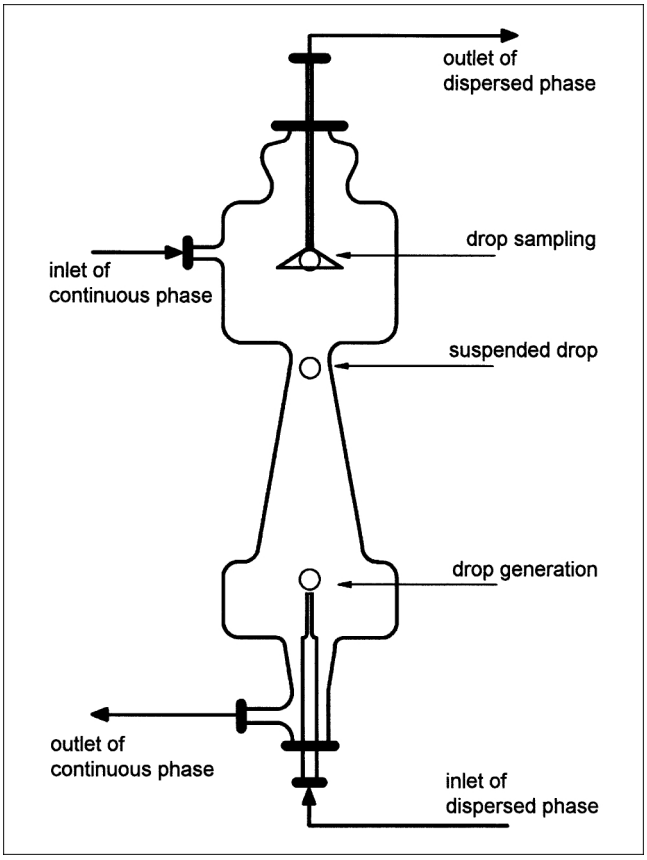

Figure 1. Single-drop cell.

Fundamental Considerations on Mass Transfer

Figure 1 shows the cell for the single-drop experiments. The mass transfer at the drop is not in steady state in the cell. When selecting a suitable model for the mathematical description of the nonstationary mass transfer from the literature, the first question to answer concerns the flow conditions inside as well as outside the droplets (at rest, laminar, or turbulent). Here unexpected difficulties already occur! While the transition from laminar to turbulent regimes at $Re \approx 2{,}300$ has been investigated extensively for pipe flow, available studies only provide information concerning the exterior of the droplets. For solid spheres at Reynolds numbers of approximately 3×10^5 the boundary layer shifts from laminar to turbulent, which results in a strong drop in the drag coefficient (see, for example, Schlichting, 1965). For small Reynolds numbers of at most 500, which occur in the single drop cell, the boundary layer should remain laminar from a hydrodynamic point of view. The vortices behind the droplets that occur at $Re \approx 100$ (depending on the viscosity ratio η_d/η_c), as observed experimentally and calculated by Brander and Brauer (1993), do not oppose the laminar flow, since they are laminar vortices. Modigell (1981) experimentally showed the laminar character of the vortices, especially the nonexistent momentum and mass transfer (except diffusive) perpendicular to the closed vortex streamlines.

The literature generally assumes a laminar outer boundary layer (see, for example, Slater (1995), and references cited there). In this case the mass-transfer resistance at the outside of the drop can be derived analytically for spherical drops:

$$Sh_c = \frac{2}{\sqrt{\pi}}\,\phi\sqrt{ReSc_c}. \tag{1}$$

Here ϕ is the correction factor that accounts for the mobility of the drop surface and that depends on the ratio of viscosities, the Reynolds number, and the contamination of the interface. According to Mersmann (1986), ϕ is 0.84 for *n*-butyl acetate drops ($d = 3.06$ mm) in water if the interface is not contaminated. For this example the mass-transfer coefficient $\beta_c = 0.000176$ m/s results outside of the drop. Even though mass transfer in the measuring cell is not in steady state, β_c does not change with time as a result of the comparably fast and continuous replacement of the phase outside the drop.

If the boundary layer outside the drop is laminar and the viscosity ratio η_d/η_c approaches unity, the flow inside the drop induced from the outside can only be weaker, or at most, the same intensity as the outside flow. Thus, there is no hydrodynamic driving force for turbulent flow inside the drop. Nevertheless, many published mass-transfer models assume turbulence (also called eddy diffusivity) inside the drop. Johnson and Hamielec (1960), Boyadzhiev et al. (1969), Steiner (1986), Slater and Hughes (1993), and Slater (1995) use an enhancement factor R' which is defined as $R' = D_{\text{eff}}/D_d$. If R' is greater than 2.5, the limiting value for laminar circulation inside the drop, this factor implies an inner turbulence. The experiments from the cited authors show that R' increases with drop radius and can reach values up to 50 or more. Handlos and Baron (1957), Olander (1966; extension of the Handlos and Baron model), and Temos et al. (1996) combine the eddy diffusivity with the inner circulation, but they give no arguments why the inner circulation is turbulent. For example, the model of Handlos and Baron (1957) which best describes experimental data, assumes that the droplet contents are completely mixed during one (hypothetically laminar) inner circulation. Such mixing completely suppresses circulation, so the circulation period actually can no longer be determined. Drops with such a turbulent internal momentum transfer should not settle noticeably faster than solid spheres, which contradicts experimental findings. Also Mersmann (1986) realizes the problems with this model assumptions, and states: "Die … Gleichung von Handlos und Baron … dürfte eher zufällig brauchbare Werte liefern" (the equation of Handlos and Baron seems to give acceptable values only by chance).

Thus, a hydrodynamic analysis suggests a mathematical model based on laminar flow at the inside of the drop corresponding to the behavior on its outside. Since no explicit analytical solution of this problem is possible, tedious numerical calculations are necessary such as those by Brauer (1979). Besides the numerical results, Brauer also presents approximate solutions for the decrease of the driving concentration difference with the time for the limiting case of $ReSc_c \to \infty$:

$$y^+ = \frac{0.289}{1+\left[\left(26.0\,Fo_d^{0.5}\right)^2+\left(3.3\cdot10^5 Fo_d\right)^2\right]^{0.5}} + 0.711\exp\left(-30.4\,Fo_d\right). \tag{2}$$

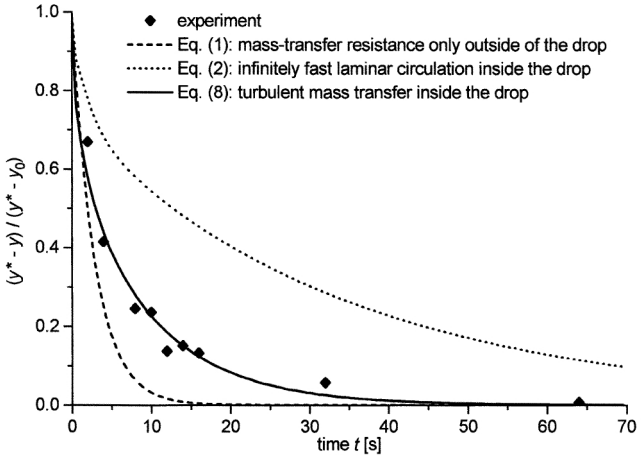

Figure 2. Measured and calculated mass transfer in single drops.

n-butyl acetate drops in water, acetone: continuous → dipsersed, $x_0 \approx 3$ wt. %, $y_0 = 0$, $d = 3.06$ mm.

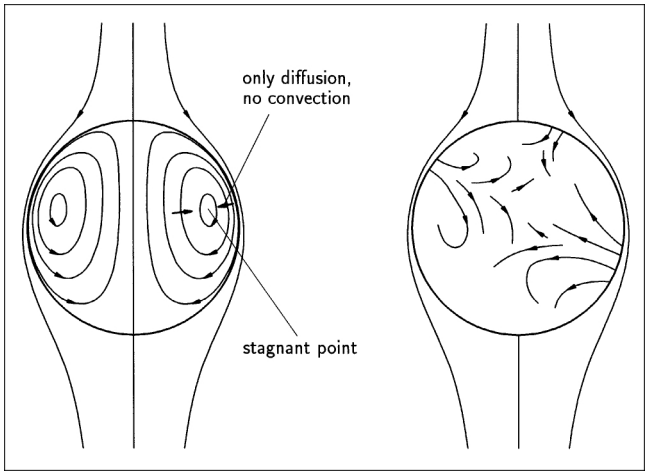

Figure 3. Concentration spreading and stream lines in a drop with infinitely fast circulation due to infinitely fast flow outside (left drop); concentration spreading in a drop if turbulent eruptions occur (right drop).

The limit $ReSc_c \to \infty$ means, for a given system, an infinitely fast flow around the drop that corresponds to an infinitely fast circulation inside the drop. In an experiment, the infinitely fast flow would of course directly lead to the onset of turbulence, but nevertheless this equation can be used to estimate an upper bound of mass transfer for laminar flow. Brauer's results are very similar to those of Kronig and Brink (1950), as well as those of Johns and Beckmann (1966). The advantage of Eq. 2 is that extensive numerical calculations are avoided.

Combining Eq. 1 with Eq. 2 in the usual way,

$$K_{od} = \frac{1}{\dfrac{1}{\beta_d \rho_d} + \dfrac{m}{\beta_c \rho_c}}, \tag{3}$$

is not done easily, since Eq. 2 is not available in β formulation. For a first comparison between theory and measurement a separate consideration of mass transfer at the inside and the outside of the drop appears advantageous. Figure 2 presents experimental data for the *n*-butyl acetate/water/acetone system together with values calculated with Eq. 1 or Eq. 2, respectively. These results provide the following conclusions:

1. Even with infinitely fast internal circulation, the driving concentration difference decreases relatively slowly (dotted line). This trend means that the mass-transfer resistance at the inside of the drop cannot be neglected. Figure 3 (left drop) gives a graphic interpretation of this finding. The infinitely fast circulation results in constant concentration along a streamline. Thus the concentration in the center of the drop is the same as at the surface. Perpendicular to the streamlines, only diffusive mass transfer can occur, and a torus forms in which the decrease in the driving concentration difference is slow (comparable to a drop without circulation).

2. Comparison of the dashed with the dotted line in Figure 2 shows that except for a very short time span the mass-transfer resistance outside of the drop is negligible compared to that at the inside, even given comparable physical properties of both phases and the distribution coefficient approaching unity. This is a result of the continuous renewal of the phase outside the drop and the behavior at the inside, according to point 1.

3. As a consequence, turbulence-like mixing occurs inside (and may occur outside) the drop. According to the previous comments, this turbulence is induced only by mass transfer and not by the hydrodynamic conditions. This turbulence must occur, since according to Eq. 2, the dotted line representing the highest possible mass transfer for the laminar case still strongly underestimates the mass transfer as measured.

A further indication of mass-transfer-induced turbulence is given by the measurements of the velocity of drop sedimentation with mass transfer, as shown in Figure 4. Drops with a diameter of 3 mm and an acetone concentration difference of

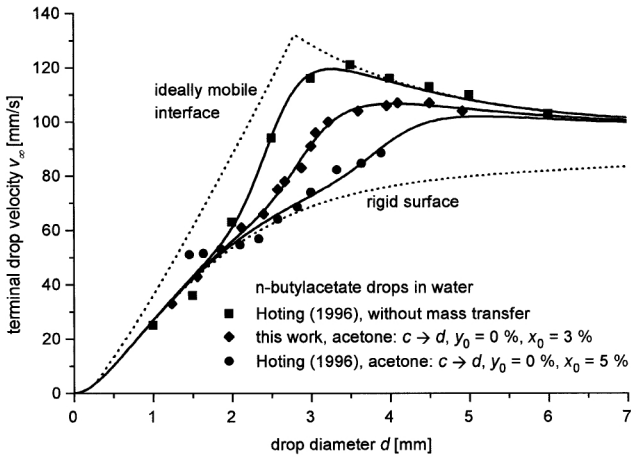

Figure 4. Influence of mass transfer on the terminal velocity of single drops.

The lines are calculated using different models (Haas et al., 1972; Ihme et al., 1972; Maneri, 1995; Modigell, 1981). The transitions from one model to the other are smoothed.

only 5 wt. % have at the start of the measurement a sedimentation velocity almost 40% below that of drops without acetone. Furthermore the measurements without mass transfer correspond to large drops almost to the limiting case of an ideally mobile interface with complete laminar internal circulation, while with increasing mass transfer, the sedimentation velocity reduces to the limiting case of a rigid interface (no internal circulation). This behavior can have two causes: (1) The interface becomes rigid because of the mass transfer; (2) Mass-transfer-induced turbulence inside the drop leads to a stochastic and irregular movement of the interface, as a result of which the drop slows, exactly as with hydrodynamically induced turbulence. Only the second reason agrees with the considerations in conclusion 3, and thus appears to be the more plausible.

After this basic discussion of mass transfer the question arises: How can this be modeled on a physically well-founded basis?

Mathematical Description of Mass Transfer in Single Drops

Table 1 lists the different mass-transfer mechanisms that correspond to the usual ranges of applicability of mass-transfer models. While diffusive mass transfer (A) and hydrodynamic–convective mass transfer (B1) have been treated quite extensively in the literature and made applicable for the engineer (see the preceding section), there are only a few first models and experimental investigations of mass-transfer-induced convective mass transfer (mechanism B2a: Orell and Westwater, 1962; Bakker et al., 1966; mechanism B2b: Davies, 1972; Wolf and Stichlmair, 1996a,b).

According to the discussion in the preceding section, it is exactly this mass transfer with mechanism B2 that is of essential importance, at least for the system investigated; our goal was to model mass transfer inside a drop based on diffusion and mass-transfer-induced turbulence. The mass-transfer resistance outside the drop will be regarded as negligible according to the above arguments. This assumption will be verified again in the following.

The model developed below uses as a basis the results of Wolf and Stichlmair (1996), who immobilized drops in a holographic interferometer by placing them between two horizontal glass plates. With this setup, they were able to visualize the turbulences inside drops. Figure 3 (right drop) shows a representation of the results. An important finding was that the turbulence spreads in the form of eruptions, starting from the interface and extending throughout the entire drop. For modeling purposes, this observation means that a turbulent exchange exists quite close to the interface. This exchange constitutes an essential difference (as compared) to the customary modeling of hydrodynamic turbulence with a laminar boundary layer close to an interface. Taking this difference into account and proceeding as usual when modeling turbulence (Glaeser and Brauer, 1977), we define

$$\epsilon_m^\sigma = \epsilon_m + \epsilon^\sigma \neq f(r). \tag{4}$$

Here ϵ^σ is a turbulent transfer coefficient that accounts for mass-transfer-induced turbulence, and ϵ_m is the turbulent transfer coefficient that accounts for hydrodynamic turbulence that may also be present. While ϵ_m depends strongly on the radius and vanishes at the interface (Glaeser and Brauer, 1977), here we assume that the sum of both coefficients is independent of radius. This assumption appears plausible according to Figure 3 (right drop). Thus for the mass-flow density of the transfer component

$$\dot{m}'' = -(D_d + \epsilon_m^\sigma)\frac{d\rho_A}{dr} \tag{5}$$

results. Since the expression in parentheses is constant, the same mathematical formulation of the time dependence of the concentration $y(r,t)$ results, as was obtained for instationary diffusion (Mersmann, 1986):

$$\frac{y^* - y(r,t)}{y^* - y_0} = \frac{6}{\pi r^+}\sum_{n=1}^{\infty}\frac{(-1)^n}{n}\sin(n\pi r^+)\exp\left[-(n\pi)^2 Fo^t\right], \tag{6}$$

with

$$r^+ = \frac{r}{R} \quad \text{and} \quad Fo^t = \frac{(D_d + \epsilon_m^\sigma)t}{R^2},$$

or averaged over the radius

$$y^+ = \frac{y^* - \bar{y}(t)}{y^* - y_0} = \frac{6}{\pi^2}\sum_{n=1}^{\infty}\frac{\exp\left[-(n\pi)^2 Fo^t\right]}{n^2}. \tag{7}$$

Here the Fourier number contains both the turbulent transfer coefficient and the diffusion coefficient, and is thus marked by the index t. A disadvantage of Eq. 7 is that for small values of t the summation has to be evaluated to high values of n to achieve convergence. The approximate solution

$$\begin{aligned} Fo^t \le 0.15: &\quad y^+ = 1 - 6\sqrt{\frac{Fo^t}{\pi}} + 3Fo^t \\ Fo^t > 0.15: &\quad y^+ = \frac{6}{\pi^2}\exp(-\pi^2 Fo^t), \end{aligned} \tag{8}$$

which represents Eq. 7 with a maximum deviation of 0.1%, is simpler to use. When applying this equation to describe experimental data, ϵ_m^σ is regarded as an adjustable parameter, since the turbulent eruptions have not yet been quantified.

Table 1. Different Mechanisms of Mass Transfer

A. Diffusive mass transfer
B. Convective mass transfer
B1. Induced hydrodynamically
B1a. Creeping flow
B1b. Laminar flow
B1c. Turbulent flow
B2. Induced by mass transfer
B2a. Laminar rolling cells
B2b. Turbulent eruption

The solid line in Figure 2 represents the results obtained for the *n*-butyl acetate/water/acetone system with a constant turbulent transfer coefficient of $\epsilon_m^\sigma = 21.5 \times 10^{-9}$ m^2/s. Thus the turbulent transfer coefficient is roughly 10 times larger than the diffusion coefficient [$D_d = 2.2 \times 10^{-9}$ m^2/s; for the physical properties, see Misek et al. (1985)]. Taking into account that laminar internal circulation can increase the mass transfer by a factor of 2.5 (Kronig and Brink, 1950), the remaining factor of 4 reflects the contribution of turbulence. Thus the enhancement factor is of the magnitude given in the literature (see previous citations).

Now it is possible to check the assumption of negligible mass-transfer resistance outside the drop. Comparison of the dashed with the solid line in Figure 2 confirms this assumption for contact times above 5 s. For shorter times, both lines give results of comparable magnitude. Thus, accounting for the mass-transfer resistance at the outside of the drop would be necessary for short times, or alternatively it has to be assumed that turbulence also occurs outside the drop. Turbulence outside the drop has been observed, as evidenced in the literature. Impressive photographs can be found in Davies (1950), von Reden et al. (1996) and Wolf and Stichlmair (1996a,b). If turbulence occurs simultaneously inside and outside the drop, the mass-transfer resistance outside will be reduced by roughly the same factor as inside due to the disturbance of the outer laminar boundary layer (see earlier). Then also for short contact times consideration of the resistance outside the drop is not necessary (at least as long as the physical properties of the phases are of comparable magnitude and the distribution coefficient approaches unity).

For modeling extraction equipment, the dependence of concentration inside the drop on drop diameter is important, as is the time dependence of the concentration. When evaluating corresponding measurements, it is found that the turbulent transfer coefficient—which is independent of time—is strongly dependent on the drop diameter. Figure 5 presents results for the *n*-butyl acetate/water/acetone system. The diameter dependence of ϵ_m^σ results from two contributions:

1. The smaller the drop diameter becomes, the smaller the turbulent eddies will be, and thus the turbulence will be increasingly damped by the viscosity of the drop phase.

2. With a smaller drop diameter, the sedimentation velocity decreases. Thus the relative velocity at the interface also decreases, which, according to Wolf and Stichlmair (1996a,b), also influences the instability of the interface.

For both reasons the mathematical description can follow the direction of Handlos and Baron (1957), since according to the previous discussion, only the *r*-dependence and the physical arguments for the turbulence differ from those of Handlos and Baron. Thus by comparison of coefficients,

$$\epsilon_m^\sigma = \frac{v_\infty d}{C_{IP}\left(1 + \frac{\eta_d}{\eta_c}\right)} \tag{9}$$

results. The constant C_{IP}, which is called the instability constant in the following, characterizes the instabilities at the interface specific to the system. C_{IP} can, in principle, take any positive value. For $C_{IP} \to \infty$, the limiting case of purely diffusive mass transfer is obtained, while $C_{IP} \to 0$ corresponds to the limiting case of infinitely fast turbulent mixing. The value of $C_{IP} = 2048$ is reached if the mass-transfer-induced turbulence lies in the range postulated by Handlos and Baron. For the example shown in Figure 5, a value of $C_{IP} = 7{,}557$ is obtained.

Since C_{IP} is a substance-specific constant, a single experimental value of $y^+(t_1, d_1)$ for a system is sufficient in principle to determine it. On the basis of this single data point, it should then be possible to calculate the concentration $y^+(t, d)$ for the transfer component for arbitrary drop diameters and contact times. Figure 6 compares calculated $y^+(t, d)$ values to experimental data for the *n*-butyl acetate/water/acetone system. In the entire range the experimental data

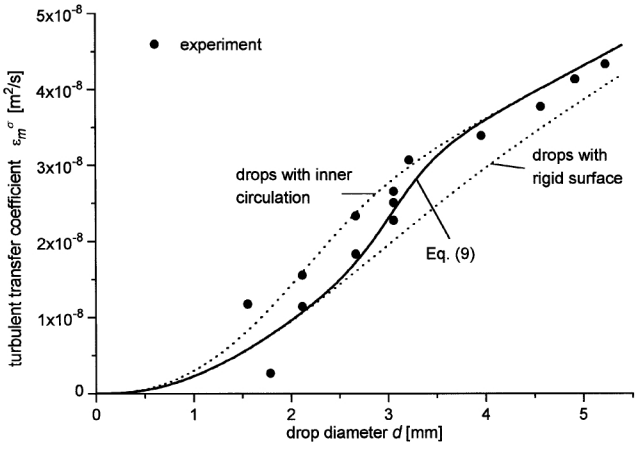

Figure 5. Dependence of the turbulent-transfer coefficient on drop diameter.

n-butyl acetate drops in water, acetone: continuous → dispersed, $x_0 \approx 3$ wt. %, $y_0 = 0$.

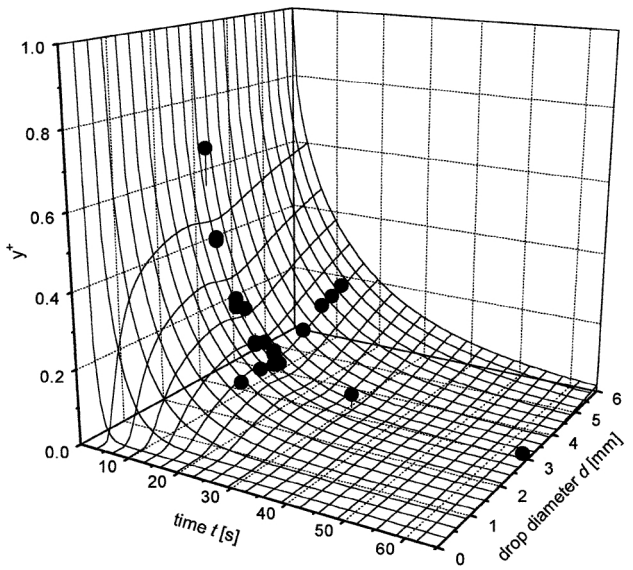

Figure 6. Decrease of the concentration difference with time in dependence on drop diameter for *n*-butyl acetate drops in water, acetone: continuous → dispersed ($x_0 \approx 3$ wt. %, $y_0 = 0$).

The vertical lines from the measured values to the mesh illustrate the deviation.

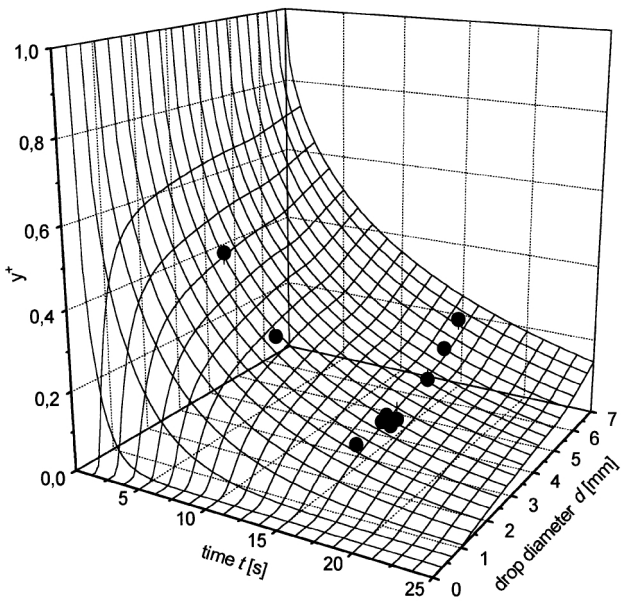

Figure 7. Decrease in the concentration difference with time in dependence on drop diameter for toluene drops in water, acetone: continuous → dispersed ($x_0 \approx 2.5$ wt. %, $y_0 = 0$).

The vertical lines from the measured values to the mesh illustrate the deviation.

agree with the values calculated on the basis of $C_{IP} = 7557$ within ± 0.02 in y^+ on the average, which compares very well with estimated experimental accuracy of less than ± 0.05 in y^+. It is interesting that, above a drop diameter of 1.5 mm, the influence of drop diameter on the concentrations is rather small. To check the applicability of the model further, experiments with the toluene/water/acetone system were carried out (for physical properties, see Misek et al., 1985). The results are presented in Figure 7. Also for this system the agreement between experimental and calculated values is as satisfactory ($C_{IP} = 7{,}389$).

It should be noted that the model dosn't take the inner circulation into account. This seems to be plausible if the inner circulation is disturbed due to the internal turbulence. If the inner turbulence is low ($\epsilon_m^\sigma \approx D_d$) and circulation occurs, other models in the literature, such as the model from Kronig and Brink, should be more suitable.

Like the model of Slater (1995), the model presented here contains only a single parameter. It must be remembered that the "contamination factor" of Slater depends not only on the components of the system but on the drop diameter and contact time as well. The instability constant in this work is substance specific, and it doesn't depend on any other parameter. Thus, it will have advantages in practical applications (such as in the design of extraction columns).

Extension of the Model for Different Boundary Conditions

One problem when transferring the results in the previous section to extraction columns is that the boundary condition of the constant concentration of the continuous phase that was implied in deriving Eq. 7 is not valid any longer (Slater, 1996). Rather, a linear change in concentration along the column corresponds to the desired profile. Unfortunately for this boundary condition, no analytical solution for the concentration profile inside the drop is available. Thus calculations are performed numerically.

The results presented in the following are based on the numerical solution of Eq. 5 for drops. The solutions were obtained with two superimposed finite-difference algorithms (FDA). In the inner FDA the drop radius is divided into 80 equidistant sections, and mass transfer is calculated for each time step from a drop's surface to its center. In the outer FDA time proceeds with a step width of 0.00004 Fo^t. From a comparison of the numerical results with Eq. 6 it could be shown that an accuracy of at least four significant digits in concentration of the transfer component can be achieved with these step sizes.

Figure 8 shows the numerical results for the concentration profiles of the transfer component in a drop. The curves are scaled to give equal average driving concentration differences, that is, the difference between the concentration at the drop surface $y^*(t)$ and the average concentration in the drop $\bar{y}(t)$. Because of this scaling, the concentration profiles hardly change above roughly $Fo^t = 0.15$, even though mass transfer is of course still taking place. The difference between the two curves shown originates from the different boundary conditions at the drop surface. For the dashed curve it is assumed that at $t = 0$ there is a jump from $y^* = 0$ to a constant surface concentration, which corresponds to the situation in the single-drop cell. For the full line a linearly increasing surface concentration, $y^* = \dot{y}_1 t$ is applied, which resembles the conditions in an extraction column. This difference between boundary conditions not only influences the concentration profiles but also the mass-transfer coefficient, the instantaneous value of which is generally defined as (Mersmann, 1986)

$$\beta_d(t) = \frac{\dot{m}''(t)}{\rho_d[y^*(t) - \bar{y}(t)]}. \tag{10}$$

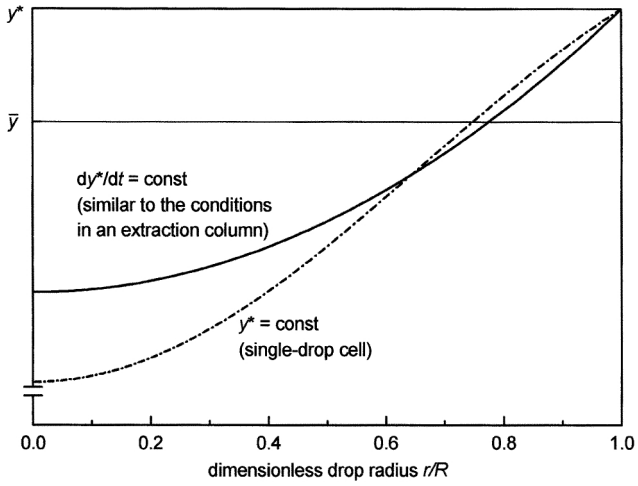

Figure 8. Concentration of the transfer component in a drop for two different boundary conditions.

The curves are normalized with respect to the driving concentration difference ($y^* - \bar{y}$).

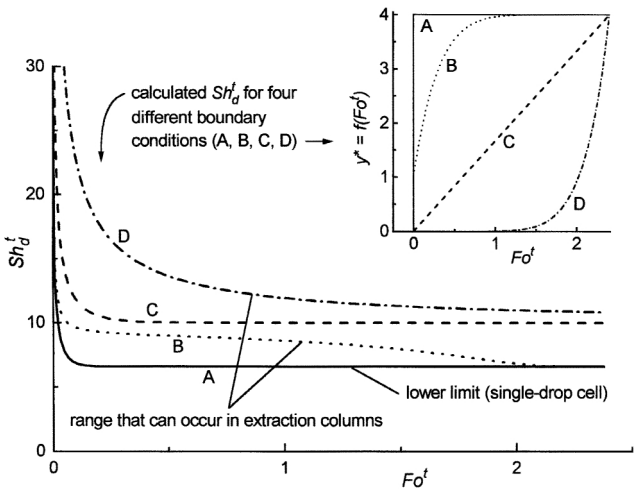

Figure 9. Dependence of mass transfer (Sh) on the concentration gradient in the continuous phase.

With $\dot{m}''$ from Eq. 5

$$\beta_d(t) = -\frac{D_d + \epsilon_m^\sigma}{y^*(t) - \bar{y}(t)} \left.\frac{dy(t)}{dr}\right|_{r=R}, \qquad (11)$$

results (that is, a direct dependence of mass-transfer coefficients on the concentration gradient at the inside surface of the drop). For the conditions shown in Figure 8,

$$\beta_d(t)|_{dy/dt=\text{const}} = 1.5\beta_d(t)|_{y=\text{const}} \qquad (12)$$

is obtained. Thus the mass-transfer coefficient obtained with a linearly increasing concentration in the continuous phase is roughly 50% larger than that which is obtained with a constant concentration (which exists in the single-drop cell). This 50% is actually only a rough estimate for long periods ($Fo^t > 0.15$) and for linear concentration gradients. Figure 9 shows the influence of different concentration gradients on mass transfer in the range that can be found in columns. The concentration profiles in the continuous phase are given as a function of time $y^*(Fo^t)$. In a column the concentration profiles are a function of the column height $y^*(h)$, but generally it can be assumed that $Fo^t \propto h$, so the profile as a function of column height can be derived from the slope of y^* as a function of time.

As a result of the calculations the instantaneous dimensionless mass-transfer coefficient inside the drop is obtained [$Sh_d^t = \beta_d(t)d/(D_d + \epsilon_m^\sigma)$]. It can be seen that, especially for short times, due to the concentration profile in the continuous phase, a quite significant increase in Sherwood number is reached as compared to the Sherwood number for a constant concentration. This finding will have to be considered for simulations of extraction columns in the future. It can be expected that the numerical results of column simulations are physically well founded only if the results of experiments with single drops are transferred to columns appropriately.

An experimental verification of these results is still difficult, because reliable models for back mixing, breakage, coalescence, and drop motion in a column are needed for the evaluation of the experimental data and for the mathematical separation of the different effects that influence mass transfer. For example, if the back mixing in a column is neglected, it is possible that a mass-transfer model that neglects the effect of the concentration gradient gives better results than a model that accounts for the concentration gradient.

An experimental proof for the transfer enhancement due to a gradient is given by Rubesin and Inouye (1973). It was shown that the local heat-transfer rates for the flow across a flat plate are 60% larger if a linear increase in the plate temperature is applied, as compared to a constant plate temperature. Taking the different geometry into account, this is in good agreement with 50% of our calculations.

Conclusions

Measured mass-transfer rates into or from liquid drops are often much larger than calculated with the theory of laminar circulation inside drops. Thus a turbulent-transfer coefficient is introduced in the transfer equations. While there is no hydrodynamic reason for the turbulent transfer, there are some arguments for a mass-transfer-induced turbulence due to interfacial instabilities. Introducing an instability parameter (C_{IP}), which is to be determined experimentally, it is possible to describe the drop size and the time dependence of the mass transfer for a given system with only one constant value of C_{IP}. The model should be used only if enhanced mass transfer (more than the model of Kronig and Brink (1950) allows) occurs.

If the results from single-drop experiments are used to calculate mass transfer in extraction columns, it is necessary to take the changed boundary conditions into account. If the concentration of the continuous phase in the single-drop cell is constant and the concentration in the column changes linearly with column height, mass-transfer enhancement of about 50% can be expected in addition to other effects, such as breakage and coalescence.

Acknowledgment

The authors thank J. Schröter and W. Bäcker from Bayer AG, Leverkusen, Germany, for supporting the experimental investigations.

Notation

A_{Tr} = surface area of the drop, m^2
d = drop diameter, m
D = diffusion coefficient, m^2/s
$Fo = (Dt/R^2)$ = Fourier number
K_{od} = overall mass-transfer coefficient related to the dispersed phase, kg/(m^2·s)
m = slope of equilibrium line ($y = mx$)
$\dot{m}$ = mass flow, kg/s
r = distance in radial direction, m
R = drop radius, m
$Re = (\rho_c v_\infty d/\eta_c)$ = Reynolds number
$Sc = (\eta/[\rho D])$ = Schmidt number
$Sh = (\beta_d/D)$ = Sherwood number
t = time, s
v_∞ = terminal drop velocity, m/s
x = mass fraction of the transfer component in the continuous phase

y = mass fraction of the transfer component in the dispersed phase

$\bar{y}$ = average value: $\bar{y} = (3/R^3)\int_0^R r^2 y \, dr$

η = viscosity, kg/(m·s)

ρ = density, kg/m^3

Subscripts and superscripts

0 = initial value

A = transfer component

c = continuous phase

d = dispersed phase

m = for momentum transfer

$*$ = equilibrium value

$+$ = dimensionless

$''$ = per unit area

t = turbulent

Literature Cited

Bakker, C. A. P., P. M. van Buytenen, and W. J. Beek, "Interfacial Phenomena and Mass Transfer," *Chem. Eng. Sci.*, **21**, 1039 (1966).

Boyadzhiev, L., D. Elenkov, and G. Kyuchukov, "On Liquid-Liquid Mass Transfer Inside Drops in a Turbulent Flow Field," *Can. J. Chem. Eng.*, **47**, 42 (1969).

Brander, B., and H. Brauer, "Impuls- und Stofftransport durch die Phasengrenzfläche von kugelförmigen fluiden Partikeln," *Fortschr.-Ber. VDI*, Series III, No. 326, VDI-Verlag, Düsseldorf (1993).

Brauer, H., "Particle/Fluid Transport Processes," *Forstchr. Verfahrenstech.*, **17**, 61 (1979).

Davies, J. T., *Turbulence Phenomena*, Academic Press, New York (1972).

Glaeser, H., and H. Brauer, "Berechnung des Impuls- und Stofftransports durch die Grenzflächen einer formveränderlichen Blase," *VDI-Forschungsheft*, No. 581 VDI-Verlag, Düsseldorf (1977).

Haas, U., H. Schmidt-Traub, and H. Brauer, "Umströmung kugelförmiger Blasen mit innerer Zirkulation," *Chem.-Ing.-Tech.*, **44**, 1060 (1972).

Handlos, A. E., and T. Baron, "Mass and Heat Transfer from Drops in Liquid–Liquid Extraction," *AIChE J.*, **3**, 127 (1957).

Hoting, B., "Untersuchung zur Fluiddynamik und Stoffübertragung in Extraktionskolonnen mit strukturierten Packungen," *Fortschr.-Ber. VDI*, Series III, No. 439, VDI-Verlag, Düsseldorf (1996).

Ihme, F., H. Schmidt-Traub, and H. Brauer, "Theoretische Untersuchung über die Umströmung und den Stoffübergang an Kugeln," *Chem.-Ing.-Tech.*, **44**, 306 (1972).

Johns, L. E., and R. B. Beckmann, "Mechanism of Dispersed-Phase Mass Transfer in Viscous, Single-Drop Extraction Systems," *AIChE J.*, **12**, 10 (1966).

Johnson, A. I., and A. E. Hamielec, "Mass Transfer Inside Drops," *AIChE J.*, **6**, 145 (1960).

Kronig, R., and J. C. Brink, "On the Theory of Extraction from Falling Droplets," *Appl. Sci. Res.*, **A2**, 142 (1950).

Maneri, C. C., "New Look at Wave Analogy for Prediction of Bubble Terminal Velocities," *AIChE J.*, **41**, 481 (1995).

Mersmann, A., *Stoffübertragung*, Springer-Verlag, Berlin (1986).

Misek, T., R. Berger, and J. Schröter, *Standard Test Systems for Liquid Extraction*, 2nd ed., The Institution of Chemical Engineers, Rugby, War., England (1985).

Modigell, M., "Untersuchung der Stoffübertragung zwischen zwei Flüssigkeiten unter Berücksichtigung von Grenzflächenphänomenen," PhD Thesis, RWTH-Aachen, Aachen, Germany (1981).

Olander, D. R., "The Handlos-Baron Drop Extraction Model," *AIChE J.*, **12**, 1018 (1966).

Orell, A., and J. W. Westwater, "Spontaneous Interfacial Cellular Convection Accompanying Mass Transfer: Ethylene Glycol–Acetic Acid–Ethyl Acetate," *AIChE J.*, **8**, 350 (1962).

Rubesin, M. W., and M. Inouye, "Forced Convection, External Flows," *Handbook of Heat Transfer*, Chap. 8, W. M. Rohsenow and J. P. Hartnett, eds., McGraw-Hill, New York (1973).

Schlichting, H., *Grenzschicht-Theorie*, 5th ed., Verlag G. Braun, Karlsruhe, Germany (1965).

Schröter, J., W. Bäcker, and M. J. Hampe, "Stoffaustauschmessungen an Einzeltropfen und an Tropfenschwärmen in einer Gegenstrommeßzelle," *Chem.-Ing.-Tech.*, **70**, 279 (1998).

Slater, M. J., "A Combined Model of Mass Transfer Coefficients for Contaminated Drop Liquid-Liquid Systems," *Can. J. Chem. Eng.*, **73**, 462 (1995).

Slater, M. J., "Liquid–Liquid Extraction Equipment: Progress and Problems," *Proc. ISEC '96*, Vol. 1, p. 35 (1996).

Slater, M. J., and K. C. Hughes, "The Application of a New Combined Film Mass Transfer Coefficient Model to the *n*-Butanol/Succinic Acid/Water System," *Proc. ISEC '93*, York, England (1993).

Steiner, L., "Mass Transfer Rates From Single Drops and Drop Swarms," *Chem. Eng. Sci.*, **41**, 1979 (1986).

Temos, J., H. R. C. Pratt, and G. W. Stevens, "Mass Transfer to Freely-Moving Drops," *Chem. Eng. Sci.*, **51**, 27 (1996).

Von Reden, C., M. J. Slater, and A. Gorak, "Aspects of Multicomponent Mass Transfer Kinetics in Liquid–Liquid Systems," *Proc. ISEC '96*, Vol. 1, p. 99 (1996).

Wolf, S., and J. Stichlmair, "The Influence of the Marangoni-Effect on Mass Transfer," *Proc. ISEC '96*, Vol. 1, p. 51 (1996a).

Wolf, S., and J. Stichlmair, "The Marangoni-Effect During Mass Transfer in Liquid–Liquid Systems," *Preprints of the 12th Int. Cong. of Chemical and Process Engineering (Chisa)*, Praha, Czech Republic (1996b).

Manuscript received Aug. 25, 1998, and revision received June 10, 1999.